The Journal of Immunology

RESEARCH ARTICLE | SEPTEMBER 15 2011

Functional Gap Junctions Accumulate at the Immunological Synapse and Contribute to T Cell Activation FREE

Ariadna Mendoza-Naranjo; ... et. al

J Immunol (2011) 187 (6): 3121–3132.
https://doi.org/10.4049/jimmunol.1100378

Related Content

Gap Junction Intercellular Communications Regulate NK Cell Activation and Modulate NK Cytotoxic Capacity

J Immunol (February,2014)

CX43 is essential for optimal cGAS function during cytosolic DNA-sensing

J Immunol (May,2018)

Gap Junction-Mediated Intercellular Communication between Dendritic Cells (DCs) Is Required for Effective Activation of DCs

J Immunol (January,2006)

Downloaded from http://journals.aai.org/jimmunol/article-pdf/187/6/3121/1348006/1100378.pdf by guest on 10 July 2024

Functional Gap Junctions Accumulate at the Immunological Synapse and Contribute to T Cell Activation

Ariadna Mendoza-Naranjo,*,†,‡ Gerben Bouma,§ Cristián Pereda,*,† Marcos Ramírez,*,† Kevin F. Webb,¶ Andrés Tittarelli,*,† Mercedes N. López,*,† Alexis M. Kalergis,‖ Adrian J. Thrasher,§ David L. Becker,¶ and Flavio Salazar-Onfray*,†

Gap junction (GJ) mediates intercellular communication through linked hemichannels from each of two adjacent cells. Using human and mouse models, we show that connexin 43 (Cx43), the main GJ protein in the immune system, was recruited to the immunological synapse during T cell priming as both GJs and stand-alone hemichannels. Cx43 accumulation at the synapse was Ag specific and time dependent, and required an intact actin cytoskeleton. Fluorescence recovery after photobleaching and Cx43-specific inhibitors were used to prove that intercellular communication between T cells and dendritic cells is bidirectional and specifically mediated by Cx43. Moreover, this intercellular cross talk contributed to T cell activation as silencing of Cx43 with an antisense or inhibition of GJ docking impaired intracellular Ca^{2+} responses and cytokine release by T cells. These findings identify Cx43 as an important functional component of the immunological synapse and reveal a crucial role for GJs and hemichannels as coordinators of the dendritic cell–T cell signaling machinery that regulates T cell activation. ***The Journal of Immunology*****, 2011, 187: 3121–3132.**

Initiation of an Ag-specific immune response requires productive engagement of TCRs by MHC-peptide (pMHC) complexes on the APC (1, 2). This TCR engagement by cognate pMHC results in the formation of a highly organized protein network known as the immunological synapse (IS), which is required for T cell activation and proliferation (3). The mature IS is characterized by the assembly of specific proteins on the T cell and APC membranes into supramolecular activation clusters. These structures consist of a centralized accumulation of TCRs and pMHC (central supramolecular activation complex [cSMAC]), surrounded by a peripheral ring (peripheral supramolecular activation complex [pSMAC]) containing the integrin LFA-1 and its receptor ICAM-1 (3, 4).

The IS is comprised of a multitude of structures, many of which are mediators of intercellular communication (5). However, it is not known whether communication involving gap junction (GJ) channels, one of the most important mechanisms for cellular cross talk, occurs at the IS assembly site. GJs are clusters of intercellular channels in the plasma membrane that mediate direct intercellular communication between adjacent cells, allowing the passage of soluble molecules, including cAMP, Ca^{2+}, ATP, inositol 1,4,5-trisphosphate, and morphogens (6, 7). GJs also mediate electrical and metabolic coupling among cells and tissues, such that signals initiated in one cell can readily propagate to neighboring cells. In mammals, functional GJs are composed of connexin (Cx) proteins. Six Cx proteins form a hemichannel (Hchl) inserted into the membrane of one cell, which then docks with a Hchl from an adjacent cell to establish a GJ channel (8, 9).

Cx- and GJ-mediated intercellular communication (GJIC) have been shown to participate in key immunological processes, such as Ig secretion and cytokine production (10), transendothelial migration of leukocytes (11), peptide transfer and cross-presentation in activated monocytes (12), activation of murine dendritic cells (DCs) (13), and regulatory T cell-mediated suppression through the transfer of cAMP (14). Additionally, we have demonstrated that GJ channels can also mediate the transfer of MHC class I-restricted melanoma peptides between human DCs, triggering T cell-specific immune response against melanoma-associated Ags (15). Recently, GJIC have also been shown to participate in DC-mediated induction of IL-2 release and proliferation of murine T cells (16). T cell activation and proliferation result from intercellular communications mediated by multiple surface molecules located at the IS. However, the accumulation of Cx at the IS, the mechanisms involved in their recruitment, and their role in T cell Ca^{2+} signaling and IFN-γ production have not been elucidated.

In the current study, we describe that Cx43, the main GJ protein of the immune system (10, 12, 17–19), accumulates at the IS and

*Institute of Biomedical Sciences, Faculty of Medicine, University of Chile, 8380453 Santiago, Chile; †Millennium Institute on Immunology and Immunotherapy, University of Chile, 8380453 Santiago, Chile; ‡University College London Cancer Institute, London WC1E 6DD, United Kingdom; §Molecular Immunology Unit, University College London Institute of Child Health, London WC1N 1EH, United Kingdom; ¶Department of Cell and Developmental Biology, University College London, London WC1E 6BT, United Kingdom; and ‖Department of Molecular Genetics and Microbiology, Millennium Institute on Immunology and Immunotherapy, Pontifical Catholic University of Chile, 8331150 Santiago, Chile

Received for publication February 11, 2011. Accepted for publication July 14, 2011.

This work was supported by Millennium Institute of Immunology and Immunotherapy Grant P09-016-F (to F.S.-O.), Chilean National Fund for Scientific and Technological Development Grants 1090238 (to F.S.-O.) and 3070036 (to A.M.-N.), European Union Marie Curie Intraeuropean Fellowship 040855 (to G.B.), and Wellcome Trust Grants 057965/Z/99/B (to A.J.T.) and 090233/Z/09/Z (to G.B. and A.J.T.).

Address correspondence and reprint requests to Dr. Ariadna Mendoza-Naranjo and Dr. Flavio Salazar-Onfray, Disciplinary Program of Immunology, Institute of Biomedical Sciences, Faculty of Medicine, University of Chile, Independencia 1027, Santiago 8380453, Chile. E-mail addresses: a.mendoza@ucl.ac.uk and fsalazar@med.uchile.cl

The online version of this article contains supplemental material.

Abbreviations used in this article: AM, acetoxymethyl; AS, antisense; cSMAC, central supramolecular activation complex; Cx, connexin; 3D, three-dimensional; DC, dendritic cell; FRAP, fluorescence recovery after photobleaching; β-Ga, 18-β-glycyrrhetinic acid; GJ, gap junction; GJIC, GJ-mediated intercellular communication; Hchl, hemichannel; IS, immunological synapse; MCL, melanoma cell lysate; pMHC, MHC-peptide; pSMAC, peripheral supramolecular activation complex; ROI, region of interest.

Copyright © 2011 by The American Association of Immunologists, Inc. 0022-1767/11/$16.00

Downloaded from http://journals.aai.org/jimmunol/article-pdf/187/6/3121/1348006/1100378.pdf by guest on 10 July 2024

mediates bidirectional cross talk between DCs and T cells in murine and human systems. Moreover, we identify a role for GJs in the regulation of T cell activation.

Materials and Methods

Mice

OT-II transgenic mice expressing the $OVA_{323–339}$ peptide (ISQAVHAA-HAEINEAGR), TCR (H-2b), and wild-type C57BL/6 mice were obtained from Charles River (Kent, U.K.). Mice were used at 6–12 wk of age, and all experiments were approved by and performed according to Home Office Animal Welfare Legislation.

Generation of DCs and T cells

This study was approved by the Bioethical Committee of Human Research, Faculty of Medicine, University of Chile. Informed written consents were given and signed by all patients. Leukocytes from stage IV melanoma patients were isolated by density gradient using Ficoll-Hypaque (Axis-Shield, Oslo, Norway). Human DCs were obtained, as described (20). At day 6, DCs were treated overnight with 150 μg/ml melanoma cell lysate (MCL), which was obtained, as previously described (15), and stimulated with 2 ng/ml TNF-α (U.S. Biological, Swampscott, MA) (MCL-DCs). DCs stimulated with 1 μg/ml LPS plus 2 ng/ml TNF-α and loaded with 2 μg/ml $gp100_{209–217}$ peptide (gp100-DCs) were used as negative control. DCs from C57BL/6 mice were cultured from bone marrow cells for 7 d in the presence of GM-CSF (20 ng/ml; Invitrogen, Paisley, U.K.). For T cell-priming experiments, DCs were maturated overnight with LPS (100 ng/ml; Sigma-Aldrich, Steinheim, Germany) in the presence or absence of OVA (100 μg/ml; Sigma-Aldrich).

MT56-4 is a $CD4^+$ T cell line derived from tumor-infiltrating lymphocyte of a melanoma patient, which specifically recognizes autologous MCL-DCs and autologous melanoma cells, and was isolated and grown, as described (15). $CD4^+$ T cells from OT-II transgenic mice were isolated from spleen using magnetic bead separation, according to manufacturer's protocol (murine $CD4^+$ T cell isolation kit; Miltenyi Biotec, Bisley, U.K.).

T cell stimulation and immune fluorescence staining

Dynal M450 beads (Dynal, Lake Success, NY) were coated with 3 μg/ml anti-human CD3 (OKT3) mAb and/or anti-human CD28 mAb (eBioscience, San Diego, CA), as well as with a control (anti-CD8) Ab (BD Pharmingen, San Jose, CA), according to manufacturer's recommendations. PBLs (2×10^4) from melanoma patients were incubated with 6×10^4 beads for 1 h at 37°C. For some experiments, PBLs were pretreated or not with 10 μM cytochalasin D (Calbiochem, Gibbstown, NJ), 5 nM latrunculin A, 10 μM taxol, or 5 μg/ml nocodazole (last three from Sigma-Aldrich) 30 min before incubation with CD3/CD28-coated beads. In this set of experiments, cells were also stained with 5 μg/ml Hoechst 33342 (Invitrogen). Polyclonal anti-Cx43 Ab (21) and/or anti-CD3 mAb, clone HIT3a (BD Pharmingen), were incubated overnight at 4°C. Samples were stained with Alexa Fluor 647 goat anti-rabbit (Molecular Probes, Invitrogen) and with tetramethylrhodamine isothiocyanate-conjugated rabbit anti-mouse (Sigma-Aldrich) and analyzed by confocal microscopy (LSM 510 META software; Carl Zeiss MicroImaging) using a ×63 NA 1.4 oil immersion objective (Carl Zeiss). The recruitment of Cx43 to the contact area was quantified, as previously described (22). Cells displaying >70% of Cx43 staining in the quadrant contacting the bead were scored as positive. One hundred T cell-bead conjugates were analyzed on ~25 fields in at least three experiments. Two independent investigators evaluated the data.

OVA-DCs or LPS-DCs (1×10^5) were coincubated for different time periods (15, 30, 45, 60, and 120 min) with 3×10^5 OT-II $CD4^+$ T cells. We allowed the conjugates to adhere to poly-*l*-lysine–coated slides, and the cell mixture was incubated with the respective primary Abs, as follows: rabbit anti-Cx43 (21); monoclonal anti-Cx43 (23); anti-Cx43Hchl, custom-made rabbit Ab raised against the extracellular loop 1 of Cx43, sequence ESAWGDEQSAFRCNTQQPGC, affinity purified (Genscript, Piscataway, NJ); biotin anti-mouse CD3 (145-2C11; BD Pharmingen); or biotin anti-mouse LFA-1 (CD11a I21/7; Leinco Technologies, St. Louis, MO). Protein expression was visualized by using the corresponding secondary fluorescence-conjugated Abs: hamster anti-mouse 7-amino-4-methylcoumarin-3-acetic acid (Jackson ImmunoResearch Laboratories, West Grove, PA), streptavidin Alexa Fluor 488 conjugate (Molecular Probes), and goat anti-rabbit DyLight 549 (Pierce, Thermo Scientific, Basingstoke, U.K.) for 1 h. Fluorescently labeled secondary Abs were added alone as negative controls. Cells were analyzed using a Leica inverted TCS SPE (Milton Keynes) confocal microscope (×40, 1.15 NA, oil immersion objective). Thirty-five conjugates/experiment were analyzed in at least three experiments.

MCL-DCs (3×10^5) were coincubated with 9×10^5 MCL-specific $CD4^+$ T cells (MT56-4) for 1 h. The cell mixture was incubated with an anti-Cx43 Ab (21). Protein expression was visualized by using the corresponding secondary fluorescence-conjugated Ab Alexa Fluor 647 goat anti-rabbit (Molecular Probes), which was also added alone as negative control. Cells were analyzed by confocal microscopy (LSM 510; ×63 NA 1.4 oil immersion objective; Carl Zeiss).

Cx43-Hchl formation was quantified by using a polyclonal anti–Cx43-Hchl Ab raised to a peptide sequence from the first external loop of Cx43 that recognizes Cx43 in an undocked conformation, and is occluded in docked GJs. T cells displaying >70% of Cx43-Hchl staining in the quadrant contacting DCs were scored as positive. We also analyzed the percentage of cells accumulated at the synapse that were not forming Hchls. To this end, a Cx43 mAb raised against the intracellular loop of Cx43 that recognized total Cx43, as both GJ and Hchls, was used, and again, T cells displaying >70% positive staining in the quadrant contacting DCs were scored as positive. We subtracted the number of cells scored as positive for Cx43-Hchl (Fig. 4*E*, dark gray) from the total number of cells scored as positive for Cx43, then obtaining the fraction of cells positive for Cx43, but negative for Hchl (Fig. 4*E*, light gray).

Three-dimensional reconstructions and projections and quantitative image analysis

The three-dimensional (3D) reconstruction of the confocal image stacks taken from interacting DCs and T cells stained for Cx43, LFA-1, and TCR was accomplished by using Volocity 4.4.0 analysis software (Improvision, Coventry, U.K.). For 3D reconstructions, ~20–25 z sections were collected at 0.3-μm *z* intervals. The en face view of the immune synapse was obtained by an *x-z* projection of the 3D image at the cellular interface of the T cell and DC. The ratio of Cx43 fluorescence at the immunological synapse versus Cx43 fluorescence at the plasma membrane was calculated using National Institutes of Health ImageJ software. Statistical analyses were carried out by the nonparametrical Mann–Whitney *U* test. The *p* values <0.05 were considered statistically significant.

Colocalization analysis

Manders's colocalization coefficients (24) were calculated at the site of interaction between OT-II T cells and OVA-DCs for TCR/Cx43, CD3/Cx43, and LFA-1/Cx43 using NIH ImageJ software with the colocalization analysis plugin JACoP. Manders's colocalization coefficient calculates the spatial overlap of two proteins, with M1 representing the percentage of Cx43 pixels (red channel) that overlaps pixels in the green channel (CD3 or LFA-1), and conversely for M2. M1 and M2 values range from 0 to 1, with a value of 0 corresponding to nonoverlapping images and the latter reflecting 100% colocalization between both images. Manders's coefficients are not influenced by differences in absolute signal intensities in each channel because pixel intensity in a particular channel is normalized to total pixel intensity across the image for that label. Values were reported as mean ± SEM.

Flow cytometry analysis

Flow cytometry experiments were performed, as previously described (15). DCs or T cells were pretreated or not with 40 μM Cx43-sense or Cx43-antisense (AS) or with 300 μM 1848 Cx43-mimetic peptide for 4 h. $CD11c^+$ cells, corresponding to DCs, were gated, and the levels of different markers, including Cx43, were analyzed using a double staining. Cells were stained using anti-Cx43 (21); PE-conjugated anti-CD11c (eBioscience); FITC-conjugated anti-CD83, CD40, MHC class I, and MHC class II (BD Pharmingen); and PE Cy5.5-conjugated anti-CD4 (eBioscience) Abs. Cells were acquired on a flow cytometer (FACSort; BD Pharmingen) and analyzed using the CellQuest software.

DC–T cell adhesion assay

OT-II T cells and OVA-DCs, pretreated or not for 4 h with 40 μM Cx43-AS or Cx43-sense (25), were coincubated for 5 or 30 min, fixed, and mounted. Images of six random fields from three individual samples per condition were taken with a ×4 0.1 NA objective on an inverted Axiovert Zeiss LSM microscope. The number of T cell–DC conjugates was quantified and reported as percentage ± SD.

Fluorescence recovery after photobleaching experiments

GJIC was quantitatively assessed in living cells by fluorescence recovery after photobleaching (FRAP) assay. Gap junctional dye transfer was measured using the acetoxymethyl (AM) ester derivative of the fluorescent indicator calcein (calcein-AM; Invitrogen). DCs interacting with T cells,

Downloaded from http://journals.aai.org/jimmunol/article-pdf/187/6/3121/1348006/1100378.pdf by guest on 10 July 2024

pretreated or not for 4 h with 40 μM murine AS (25) or human Cx43-AS (sequence: 5′-GTAATGCGGCAAGAAGAATTGTTTCTGTC-3′), 40 μM Cx43-sense (25), 300 μM Gap20 control peptide, 300 μM 1848-mimetic peptide, or 50 μM 18-β-glycyrrhetinic acid (β-Ga) were collected and loaded with 1 μM calcein-AM in culture medium for 30 min. Once inside the cell, endogenous esterases cleave the lipophilic AM groups, producing fluorescent calcein molecule that is unable to leak out of cells across cell membranes, but is able to pass between cells connected via GJs.

FRAP was performed on a Leica SPUV (Milton Keynes) confocal microscope (×40, 0.8 NA, water immersion objective), using the FRAP function on the Leica confocal software, 1 h after calcein-AM loading. As a control, 1 mM propidium iodide was added to the media to check cell viability during imaging. A region of interest (ROI), either the T cell or the DC, was chosen, and between 12 and 15 cycles of the 488 nM laser at 12% emission strength were used to photobleach the fluorescence within the ROI. These were the conditions determined for optimal bleaching of the DC–T cell conjugates. The progression of FRAP was followed by continuously acquiring images with a time interval of 5 s for 2 min of total imaging time. Fluorescence of the mobile fraction was quantified using the mean ROI function (ImageJ software). Fluorescence intensities of ROIs were recorded before photobleaching, immediately after photobleaching, and at 5-s intervals after photobleaching. The percentage of fluorescence recovery was calculated using the equation for determining the mobile fraction (26).

Measurement of Ca^{2+} signals

A Leica SPUV confocal microscope (×63, 1.2 NA, water immersion objective) was used for analysis of Ca^{2+} transients in MCL-specific $CD4^+$ T cells cocultured with MCL-DCs, as well as in OVA-DCs incubated with OT-II T cells. Cells pretreated or not for 4 h with 40 μM Cx43-AS, 40 μM Cx43-sense, 300 μM Gap20 control peptide, 300 μM 1848-mimetic peptide, or 50 μM β-Ga were collected and stained with 1 μM Fluo4-AM (Molecular Probes, Invitrogen). The 1848-mimetic peptide and Gap20 control peptide were added back after washing the cells to remove excess probe. The Fluo4-AM fluorescence and bright field were monitored simultaneously by taking frames at 10-s intervals. Intracellular Ca^{2+} signals were reported as total mean fluorescence ± SEM and were quantified as Fluo4 fluorescence at any time point-basal fluorescence obtained by averaging all the frames. The emission intensity was displayed on a pseudocolor scale using the Leica Lite browser software.

IFN-γ ELISPOT assay

MultiScreen plates (MAPN1450; Millipore, Watford, U.K.) were coated overnight with 2 μg/ml anti-human IFN-γ capture mAb (1-D1K; Mabtech, Stockholm, Sweden). MCL-DCs and autologous MCL-specific $CD4^+$ T cells were preincubated for 4 h in the presence or absence of 300 μM 1848 Cx43-mimetic peptide (sequence CNTQQPGCENVCY extracellular loop 1; 95% purity), 300 μM Gap20 control peptide (EIKKFKYGIEEHC cytoplasmic loop; 95% purity) (both from JPT Peptide Technology, Berlin, Germany), 50 μM β-Ga, 40 μM Cx43-AS, or vehicle. After this time, 5×10^3 DCs were cocultured with T cells at a 1:1 ratio for another 4 h. Additionally, nontreated DCs and T cells were coincubated cells at a 1:1 ratio for another 4 h with T cells and DCs, respectively, which were pretreated 4 h with the aforementioned drugs or vehicles. IFN-γ spots were counted using an automated counter ELISPOTscan (A.EL.VIS, Hannover, Germany).

Statistics

Statistical analysis was done using the Statgraphics-Plus 2.1 software. Differences between treatments were tested by one-way ANOVA, using Duncan's multiple comparison procedure or the Mann–Whitney *U* test for data sets of multiple comparisons. Results are presented as mean ± SD, except where stated. The p values <0.05 were considered statistically significant.

Results

Cx43 accumulation at the T cell stimulatory interface is dependent on the actin cytoskeleton

Beads coated with Abs directed against CD3 and the costimulatory surface receptor CD28 have been widely used to mimic T cell activation by APCs. Cx43 was found to accumulate at the site of contact formed between T cells and beads after stimulation with anti-CD3 and anti-CD28 beads, whereas a random distribution of Cx43 was observed in T cells incubated with beads coated with an irrelevant Ab (Fig. 1*A*). Image analysis confirmed that >60% of T cells recruited Cx43 following activation with anti-CD3 plus anti-CD28 beads (Fig. 1*B*). In contrast, only 30% of T cells accumulated Cx43 in the presence of anti-CD3– or anti-CD28–coated beads, similar to what was found when using an irrelevant Ab (Fig. 1*B*). Furthermore, accumulation of Cx43 and CD3 was found following T cell engagement, suggesting that Cx43 may be recruited to the stimulatory synapse formed between T cells and APCs (Fig. 1*C*).

As recent work has provided evidence for direct targeting of Hchl to cell-cell junctions through a pathway that is dependent on microtubules (27), we investigated whether Cx43 recruitment after TCR engagement was a cytoskeleton-dependent process. The distribution of Cx43 was analyzed by confocal microscopy in human $CD4^+$ T cells, which were incubated with anti-CD3 and anti-CD28 beads in the presence or absence of specific inhibitors of either microtubule or actin polymerization. When microtubule dynamics were inhibited by incubation with taxol or nocodazole, similar accumulation of Cx43 at the site of contact was observed as in the absence of inhibitors (Fig. 2*A*, 2*B*, 2*D*). In contrast, incubation with either latrunculin A or cytochalasin D (inhibitors of actin polymerization) completely abrogated Cx43 accumulation to the contact area (Fig. 2*C*, 2*D*). These results indicate that Cx43 recruitment to the synapse is dependent on the actin cytoskeleton.

Cx43 accumulates at the IS pSMAC in an Ag-specific and time-dependent manner

Cx43 distribution was then investigated by confocal microscopy in conjugates of human DCs loaded with a MCL and cocultured with $CD4^+$ T cells that specifically recognize autologous MCL-DCs (Supplemental Fig. 1*A*). Cx43 was found to accumulate to the interface between T cells and MCL-DCs (Fig. 3*A*, arrowhead), but was homogeneously distributed when T cells were incubated with DCs pulsed with the control Ag gp100 (Fig. 3*A*). As the MCL contains a number of unknown antigenic peptides, Cx43 accumulation was further investigated using $CD4^+$ T cells from OT-II mice, which carry a transgenic TCR specifically recognizing the $OVA_{323–339}$ peptide presented in MHC class II. OT-II $CD4^+$ T cells were coincubated with mature bone marrow-derived DCs (LPS-DCs) or OVA-pulsed mature DCs (OVA-DCs), and synapse formation was visualized by confocal microscopy. Cx43 was found to accumulate at the synapse formed between OT-II T cells and OVA-DCs (Fig. 3*B*, arrowhead), but was almost completely absent when T cells were incubated with LPS-DCs (Fig. 3*B*). Quantification showed that >60% of OVA-DC and OT-II T cell conjugates concentrated Cx43 at the T cell–DC interface, and a 4-fold increase of Cx43 accumulated at the contact area, compared with the plasma membrane (Fig. 3*C*). Similar amounts of Cx43 recruited to the MCL-DCs and MCL-specific T cell interface, and a 3-fold increase of Cx43 accumulated at the contact area was observed when using the human model (Fig. 3*C*). In contrast, in the absence of Ag-specific presentation (LPS or gp100), fewer conjugates accumulated Cx43, and reduced Cx43 amounts were found at the site of T cell–DC interaction (Fig. 3*A–C*).

Spatial segregation of accumulated molecules at the IS leads to the formation of cSMAC and pSMAC within the synapse (4). To establish to which compartment Cx43 was recruited, the distribution of Cx43 was compared with the distribution of CD3 (cSMAC) and LFA-1 (pSMAC). The Cx43 pool that redistributed to the IS was only partially colocalized with CD3 (Fig. 3*E*, Supplemental Fig. 1*B*), and was found predominantly colocalized with LFA-1 (Fig. 3*F*, Supplemental Fig. 1*C*) in both mouse and human models, indicating a preferential recruitment of Cx43 to the

Downloaded from http://journals.aai.org/jimmunol/article-pdf/187/6/3121/1348006/1100378.pdf by guest on 10 July 2024

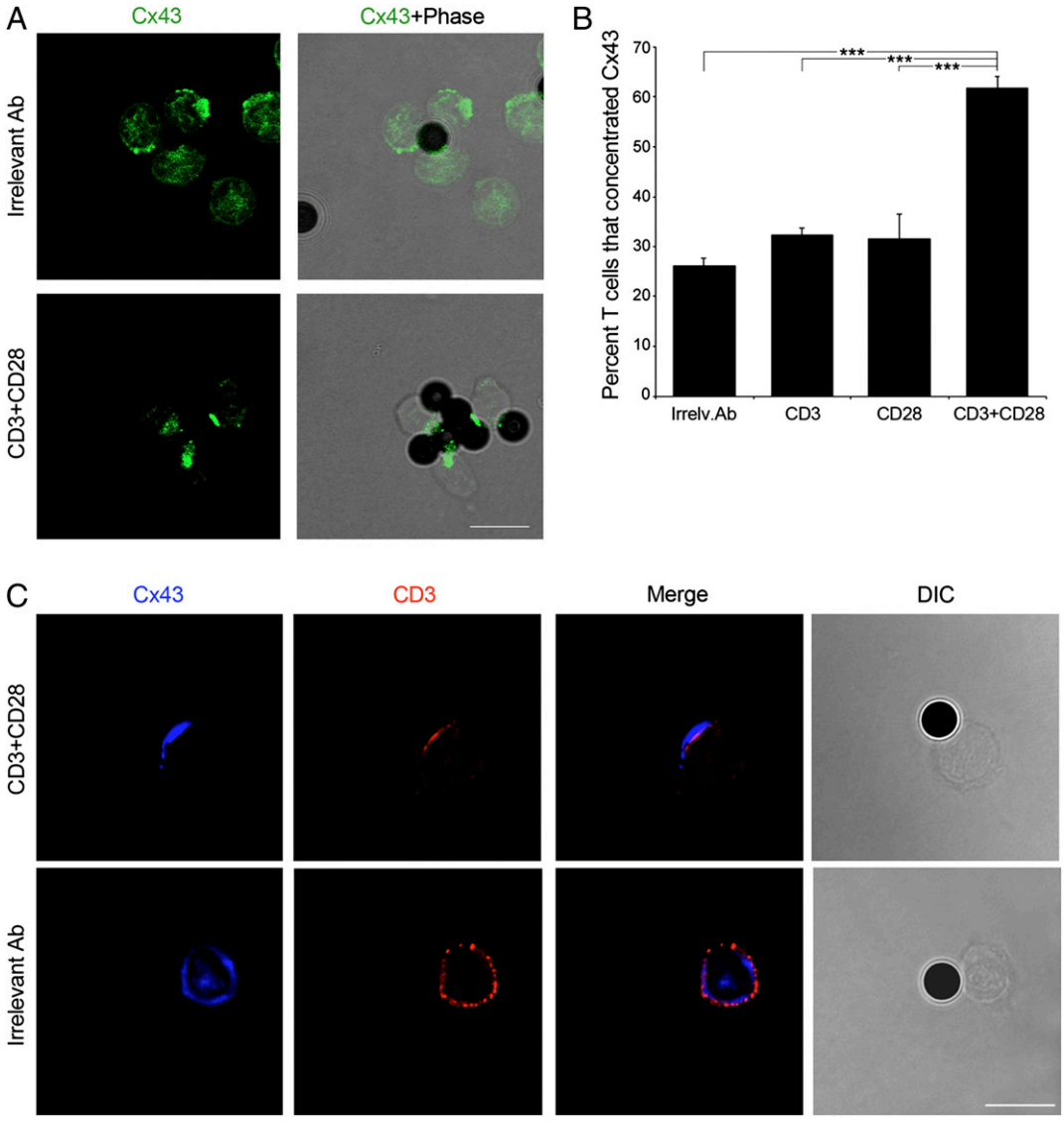

FIGURE 1. Costimulatory signals induce Cx43 accumulation at the contact site. *A*, Cx43 distribution was analyzed in T cells stimulated with magnetic beads coated with anti-CD3 and anti-CD28, or with an irrelevant Ab. Scale bar, 10 μm. *B*, The number of T cells that accumulate Cx43 at the site contacting the beads was quantified under the different conditions studied. Values are expressed as the percentage of cells that polarized Cx43 to the contact site, relative to the total number of cells examined. Each plotted point represents mean ± SD of four independent experiments. Differences are indicated by *p* values (***$p < 0.005$). *C*, The distribution of Cx43 and CD3 was analyzed by confocal microscopy in T cells stimulated with magnetic beads coated with an irrelevant Ab or with anti-CD3 plus anti-CD28. Images are representative of three independent experiments. Scale bar, 10 μm.

pSMAC ring. This observation of colocalization was calculated by quantification using overlap coefficient according to Manders's automatic threshold determination. Cx43 displayed 63.1% colocalization with LFA-1, against only 35.7% with CD3. The measured colocalization coefficients for Cx43-LFA-1 and LFA-1-Cx43 were statistically higher ($p < 0.05$) compared with the values for Cx43-CD3 and CD3-Cx43 (Fig. 3*D*).

Furthermore, serial optical sections along the *z*-axis for Cx43, LFA-1, and TCR labeling on OVA-DCs or LPS-DCs contacting OT-II T cells were taken, allowing 3D reconstruction and projection on the *x*-*z* plane. Fig. 3*G* shows representative en face views illustrating the Cx43 accumulation at the DC–T cell interface. Whereas the TCR clustered in the central zone of a T cell in contact with an OVA-DC, Cx43 was excluded from this area and was found coclustering with LFA-1 at the peripheral zone of contact (Fig. 3*G*). Cx43 accumulation was rare at the site of interaction of conjugates formed between OT-II T cells and LPS-DCs (Fig. 3*G*).

The molecular structure of the IS facilitates Ag recognition and T cell activation. To further investigate whether accumulation of Cx43 at the synapse is Ag specific, as well as to evaluate dynamic changes in Cx43 recruitment, the distribution of Cx43 was analyzed over time in both mouse and human systems. Accumulation of Cx43 to the contact area of DCs interacting with T cells was quantified and analyzed, as previously described (22). Significant higher recruitment of Cx43 to the IS was found in conjugates of OT-II T cells and OVA-DCs (Fig. 4*A*, 4*B*, $p < 0.01$ and $p < 0.005$; Supplemental Fig. 2*A*, $p < 0.05$). Maximal accumulation of Cx43 was observed 30–45 min after OT-II T cell/OVA-DC incubation (Fig. 4*B*, 4*C*), whereas in the human model statistically significant differences were observed 45 min after MCL-DC and MCL-specific T cell incubation (Supplemental Fig. 2*A*). In contrast, when OT-II T cells were incubated with LPS-DCs, or when MCL-specific T cells were cocultured with gp-100-DCs, substantially fewer conjugates accumulated Cx43 at the site of interaction (Fig. 4*A*–*C*, Supplemental Fig. 2*A*). Taken together, these data identify

Downloaded from http://journals.aai.org/jimmunol/article-pdf/187/6/3121/1348006/1100378.pdf by guest on 10 July 2024

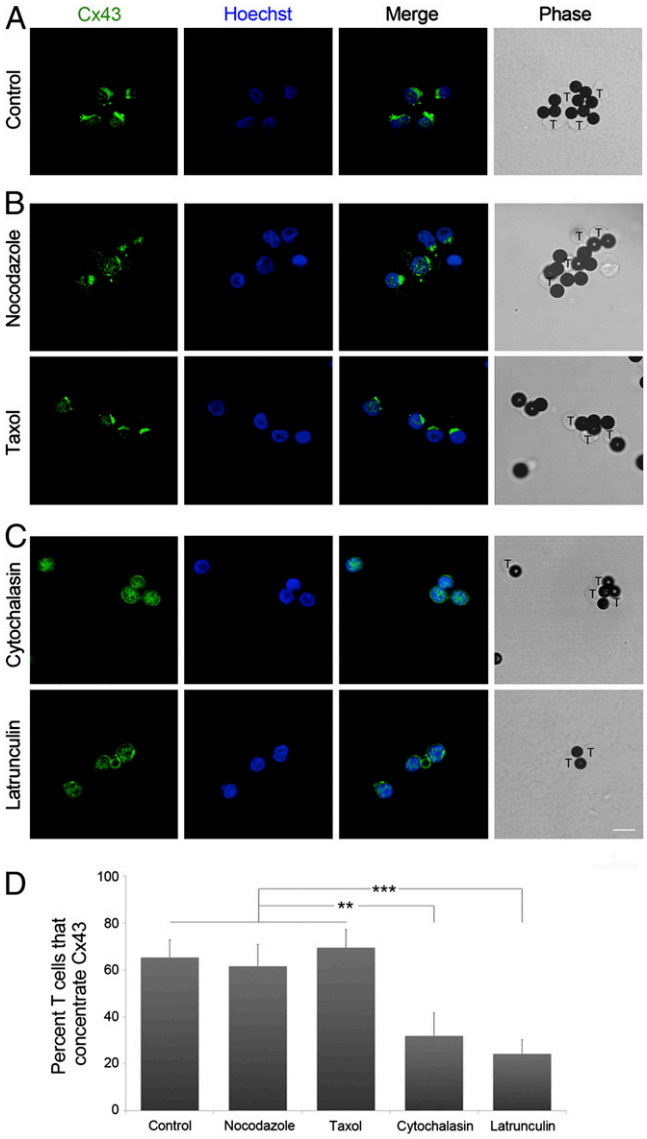

FIGURE 2. Recruitment of Cx43 is an actin-dependent process. PBLs were incubated for 30 min in the presence or absence (*A*) of taxol or nocodazole (*B*), or cytochalasin D or latrunculin A (*C*), before incubation with CD3- and CD28-coated beads. Cx43 and Hoechst staining were analyzed by confocal microscopy. The inducible capping of Cx43 to the contact area was impaired in the presence of the inhibitors of actin polymerization. Scale bar, 10 μm. *D*, The number of T cells that accumulate Cx43 at the site contacting the beads was quantified under the different conditions studied. Values are expressed as the percentage of cells that recruit Cx43 to the IS, relative to the total number of cells examined. Differences are indicated by *p* values (**$p < 0.01$, ***$p < 0.005$).

Cx43 as a component of the IS, and suggest that Cx43 recruitment is time dependent and requires cognate Ag recognition by T cells.

Cx43 accumulates at the IS as Cx Hchls

Besides GJs, Cx can also form stand-alone Hchls; therefore, we analyzed whether Hchls may possibly form and accumulate to the IS. To address this, a polyclonal anti–Cx43-Hchl Ab raised to a peptide sequence from the first external loop of Cx43 that recognizes Cx43 in an undocked conformation, and is occluded in docked GJs, was used to examine the distribution of Hchls in conjugates of T cells and DCs in both mouse and human systems. This Cx43-Hchl Ab was used in combination with a Cx43 mAb raised against the intracellular loop of Cx43 (23). Cx43-Hchl formation and synapse accumulation were confirmed in human and mouse DC–T cell conjugates (Fig. 4*D*, Supplemental Fig. 2*B*). Significant accumulation of Cx43 Hchls was found at the interface of OT-II T cells and OVA-DCs, compared with LPS-DCs, 30 min after conjugate formation (Fig. 4*E*, $p < 0.05$ and $p < 0.01$), and a 2-fold increase of Cx43 accumulated at the contact area, compared with the plasma membrane, was observed 2 h after cognate $CD4^+$ T cell–DC interaction in both human and mouse model (Fig. 4*F*, Supplemental Fig. 2*C*, 2*D*). These data provide evidence for Cx43 accumulation at the IS as stand-alone Hchls.

GJs mediate bidirectional communication between DCs and T cells

Bidirectional communication mediated by GJs between cells of the immune system has been previously described (10). The establishment of bidirectional GJIC between DCs and T cells was then monitored by FRAP. OT-II T cells and DCs were loaded with calcein-AM, a fluorescent GJ channel permeant dye, and bleached, and the recovery of fluorescence was monitored for 2 min at intervals of 5 s. Cell viability was verified by propidium iodide exclusion, which was added to the medium and was present throughout the experiment. Cell communication from DCs to T cells, identified as fluorescence recovery, was confirmed 2 min after bleaching OT-II T cells forming conjugates with OVA-DCs (Fig. 5*A*, 5*C*, 5*D*, Supplemental Video 1). Bidirectional transport, in this case from T cells to DCs, was observed when OVA-DCs were photobleached and fluorescence recovery monitored (Fig. 5*B*, 5*D*, Supplemental Video 2). In contrast, photobleaching of T cells contacting LPS-DCs, or bleaching of LPS-DCs contacting OT-II T cells showed no fluorescence recovery (Fig. 5*A–D*), indicating that this is an Ag-dependent process. Inhibiting Cx43 by means of a Cx43-AS oligodeoxynucleotide that targets Cx43 expression in T cells and DCs (Supplemental Fig. 3*A–D*) completely blocked fluorescence recovery (Fig. 5), confirming that Cx43 is required for functional GJs to form in either direction. In contrast, intercellular communication was not affected when DC–T cell conjugates were incubated with a Cx43-sense oligo control (Supplemental Fig. 3*E*, 3*F*). We also investigated fluorescence recovery after incubation with β-Ga or the Cx43-mimetic peptide 1848 that blocks docking between adjacent Hchls. Intercellular communication was dramatically reduced after treatment with these inhibitors, although was not affected in cells treated with the Gap20 control peptide (Supplemental Fig. 3*E*, 3*F*).

Moreover, FRAP analysis using MCL-specific T cells and DCs confirmed our findings in the human model (Supplemental Fig. 3*G*, 3*H*). These results provide support for the role of Cx43 in mediating bidirectional intercellular communication between T cells and DCs at the IS.

Cx43 is required for APC-mediated T cell activation

Binding of TCR to specific MHC-peptide complexes triggers downstream intracellular events and oscillations of intracellular Ca^{2+}, essential for T cell activation (28). Because previous studies have described Cx43 participation in Ca^{2+} influx in various cell types (29, 30), we investigated whether Cx43 was involved in regulating Ca^{2+} signaling in T cells. Calcium signals were monitored over time in T cells coincubated with MCL-DCs and loaded with Fluo4-AM. Ag-specific T cell stimulation resulted in oscillation of intracellular Ca^{2+}, which was impaired when DCs and T cells were preincubated and cocultured in the presence of the different GJ or Cx43 inhibitors (Fig. 6*A–C*). When the Ca^{2+} influx was analyzed in the murine OT-II model system, similar findings were obtained (Supplemental Fig. 4*A*, 4*B*).

No differences were detected in the expression of MHC class I and class II, CD40, and CD83 when DCs were cultured in the

Downloaded from http://journals.aai.org/jimmunol/article-pdf/187/6/3121/1348006/1100378.pdf by guest on 10 July 2024

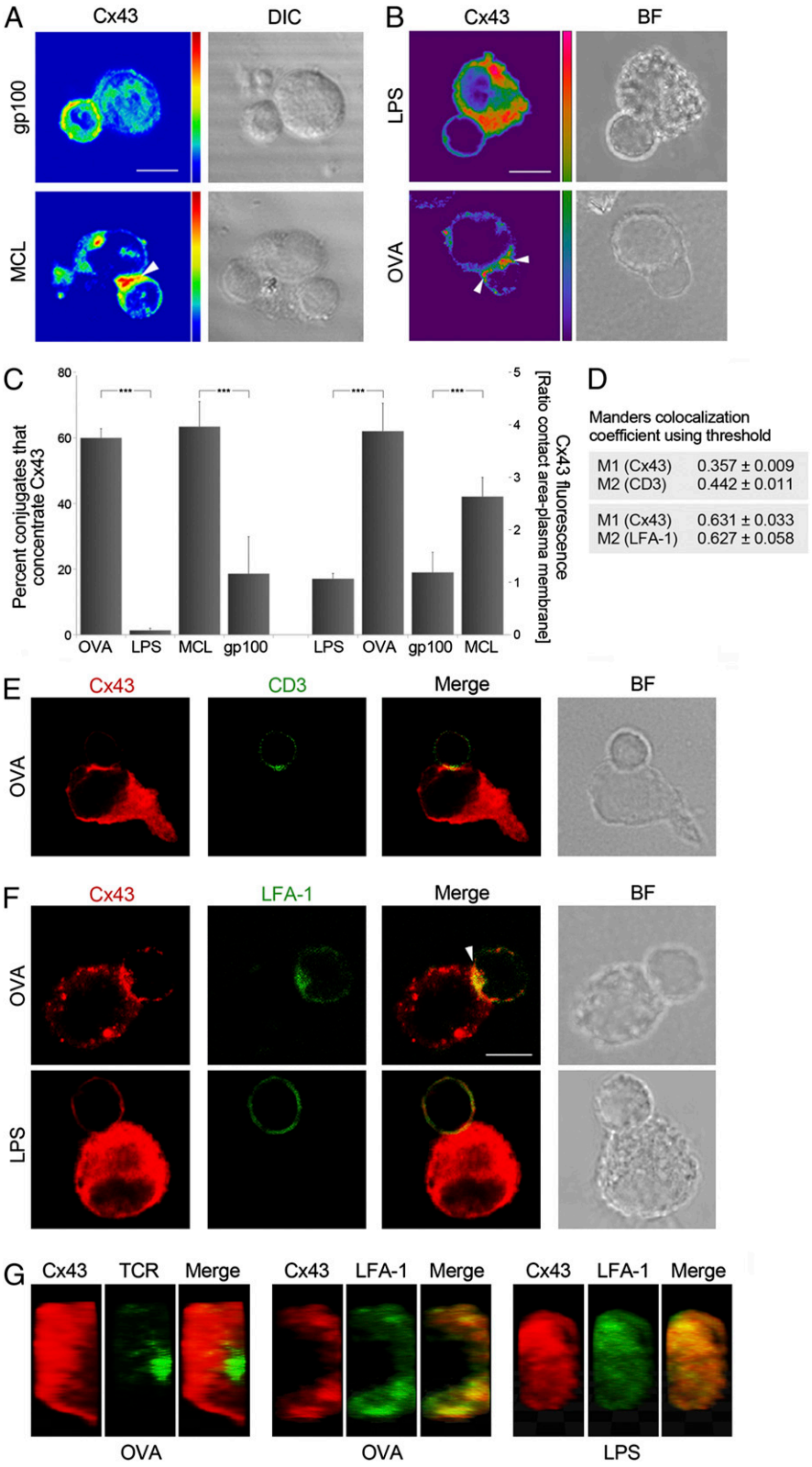

FIGURE 3. Cx43 is recruited to the IS and accumulates preferentially in the pSMAC between T cells and DC. Cx43 accumulates at the site of interaction of MCL-DCs and MCL-specific T cells (arrowhead) (*A*), and OVA-DCs and OT-II $CD4^+$ T cells (arrowheads) (*B*), but distributes homogeneously in T cells incubated with gp100-DCs and LPS-DCs (*A* and *B*, respectively). Scale bar, 5 μm. *C*, The number of T cells that accumulate Cx43 at the site of contact, and the ratio of Cx43 fluorescence accumulated at the contact area versus at the plasma membrane was quantified. Values are expressed as mean ± SD of three independent experiments. Differences are indicated by p values (***$p < 0.005$). *D*, The colocalization coefficients for Cx43 (M1 channel) and for CD3 or LFA-1 (M2 channel) were calculated using Manders's automatic threshold determination. Manders's coefficients range from 0 (no overlap) to 1 (complete overlap). Values appear indicated as mean ± SEM. Cells were costained for Cx43, and CD3 (*E*) and LFA-1 (*F*) distribution was evaluated by confocal microscopy in conjugates of OVA-DCs (or LPS-DCs, in *F*) and OT-II T cells. Cx43 was found partially colocalizing with CD3 (*E*) and was mainly accumulated in the pSMAC within the IS (*F*, arrowhead). Scale bar, 5 μm. *G*, En face views illustrating the Cx43 accumulation at the DC–T cell interface in a 0.5-μm confocal layer. Cx43 was preferentially concentrated in the peripheral (pSMAC) area of the immunological synapse.

presence of Cx43 inhibitors (Fig. 6*D*). Moreover, incubation with the Cx43-AS did not alter the expression of TCR complexes on T cells (Fig. 6*E*). These data indicate that inhibition of GJIC does not affect signals 1 and 2 of T cell activation; therefore, the impairment in Ca^{2+} signaling is most likely the result of reduced GJ or Hchl activity.

As interactions between opposing GJ Hchls are a form of intercellular adhesion, the contribution of Cx43 to adhesion of T cells and Ag-pulsed DCs was also investigated. Silencing of Cx43 did not substantially alter cell adhesion, and similar numbers of conjugates were formed between untreated, Cx43-AS–, and Cx43-sense–treated cells (Fig. 6*F*).

To further investigate whether recruitment of Cx43 to the IS contributes to T cell activation, the secretion of IFN-γ was evaluated by ELISPOT after both T cells and DCs were incubated (or not) with β-Ga, the 1848 Cx43-mimetic peptide, Cx43-AS, or

Downloaded from http://journals.aai.org/jimmunol/article-pdf/187/6/3121/1348006/1100378.pdf by guest on 10 July 2024

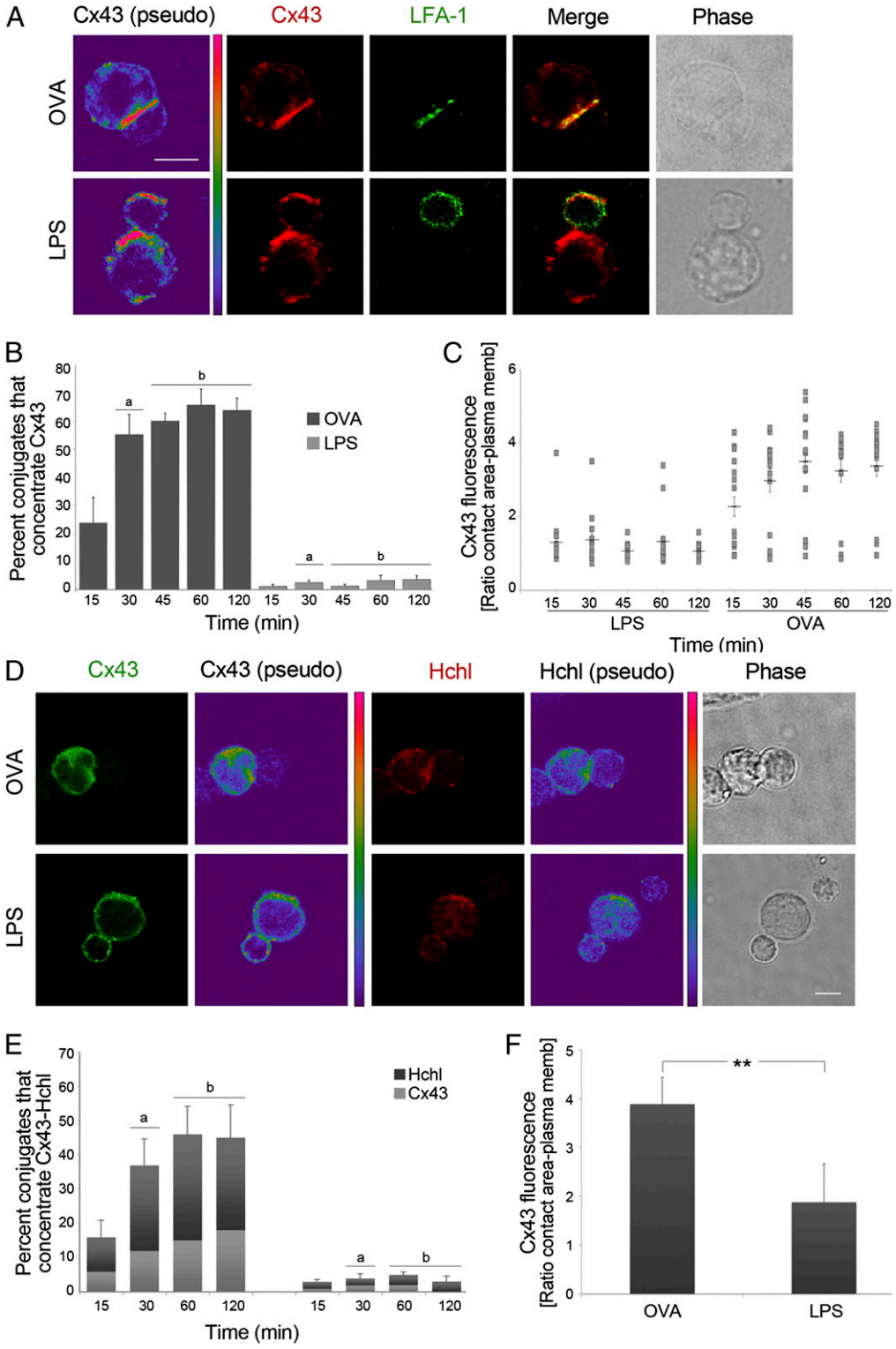

FIGURE 4. Cx43 and Cx43-Hchls accumulate at the IS in a time-dependent and Ag-specific way. *A*, Representative images of Cx43 and LFA-1 distribution after incubation of OVA-DCs or LPS-DCs with OT-II T cells are shown. Scale bar, 5 μm. *B*, Cx43 accumulation at the IS was evaluated at different time points based on positive costaining of Cx43 and LFA-1 in OVA-DCs or LPS-DCs cocultured with OT-II T cells. Each plotted point represents mean ± SD of three independent experiments (*a*, $p < 0.01$ and *b*, $p < 0.005$). *C*, Cx43 distribution to the synapse was measured as ratio of Cx43 accumulated at the contact site versus at the plasma membrane, and was evaluated at different time points. Cx43 accumulation was significantly higher in T cells cocultured with OVA-DCs versus LPS-DCs (30 min, $p < 0.01$; 45, 60, and 120 min, $p < 0.005$). Values are expressed as mean ± SEM; $n = 3$. *D*, Hchls and Cx43 accumulate at the site of interaction of OVA-DCs and OT-II $CD4^+$ T cells, but distribute randomly in T cells incubated with LPS-DCs. Scale bar, 5 μm. *E*, The percentage of cells that accumulated Hchls (dark gray) and Cx43 (light gray) at the synapse was assessed. Values are reported as mean ± SEM (*a*, $p < 0.05$ and *b*, $p < 0.01$). *F*, The ratio of Cx43 fluorescence accumulated at the contact area versus at the plasma membrane was quantified 2 h after DC-T cell conjugate formation. Values are expressed as mean ± SD of three independent experiments. Differences are indicated by *p* values (**$p < 0.01$).

Downloaded from http://journals.aai.org/jimmunol/article-pdf/187/6/3121/1348006/1100378.pdf by guest on 10 July 2024

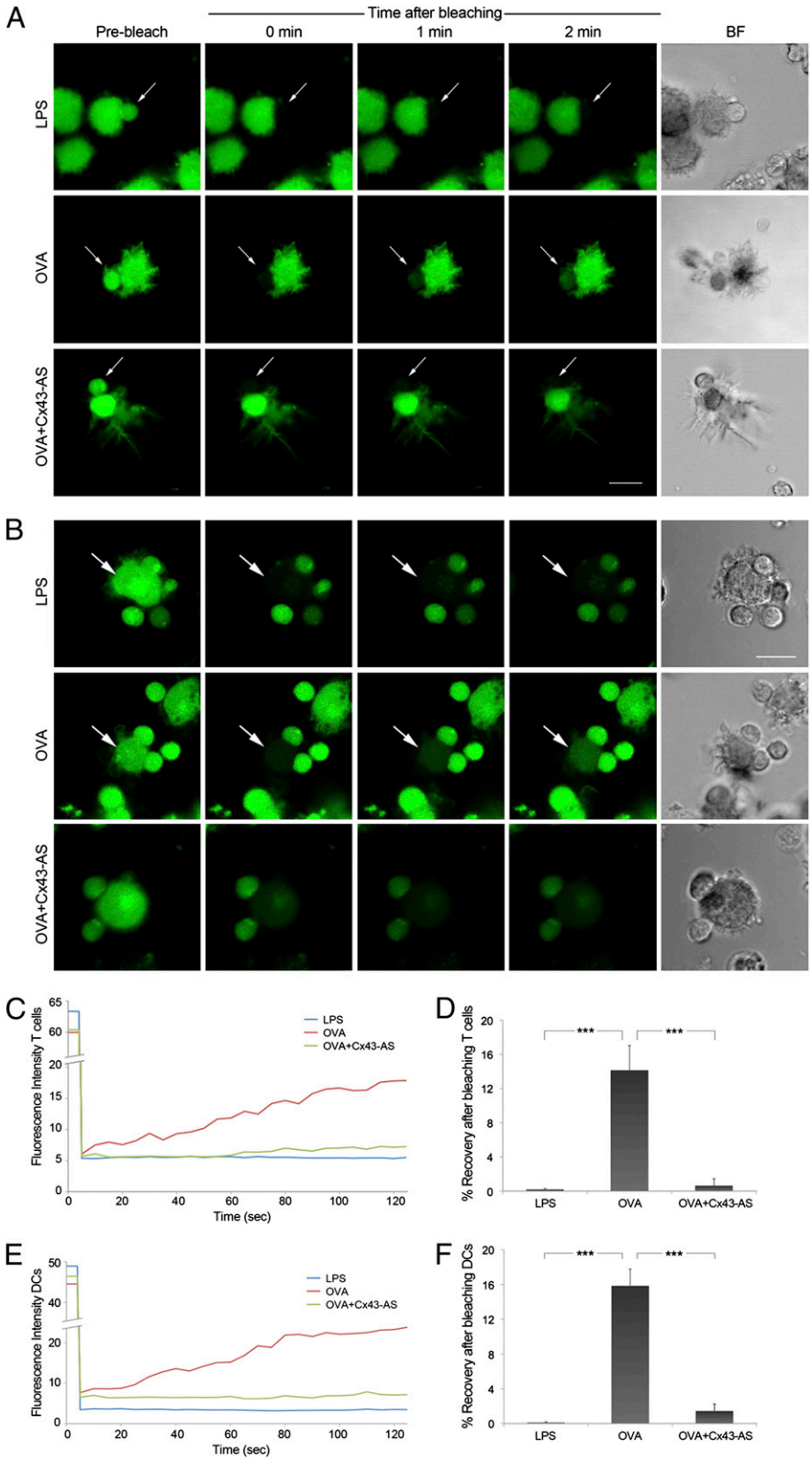

FIGURE 5. DCs and T cells communicate through functional GJs. *A*, FRAP experiments were carried out in conjugated formed between LPS-DCs or OVA-DCs and OT-II T cells. Cocultures of OVA-DCs and T cells pretreated 4 h with a Cx43-AS were also analyzed. After loading both cell populations with calcein-AM (green), T cells were bleached and the fluorescence recovery was monitored over a period of 2 min. Representative images of fluorescence restoration (or not) and bright field (BF) images are shown. Arrows indicate the target cell before and after photobleaching. Scale bar, 10 μm. *B*, OVA-DCs or LPS-DCs, and OT-II T cells were loading with calcein-AM (green), DCs were bleached, and the fluorescence recovery in the photobleached region was monitored over a period of 2 min. Representative images of fluorescence restoration (or not) and bright field images corresponding to the same fields are shown. Arrows indicate the target cell before and after photobleaching. Scale bar, 10 μm. *C* and *E*, Representative fluorescence recovery curves for T cells and DCs, respectively, illustrating the kinetic profile for each condition, are shown. Recovery was confirmed only between OVA-DC and OT-II T cell conjugates and was negative for the other conditions. *D* and *F*, Data were analyzed to show the incidence of dye coupling after photobleaching of T cells or DCs, respectively. Mean values were expressed as percentage ± SEM (***$p < 0.005$); $n = 3$.

their respective controls. T cell activation was significantly reduced after incubation with each of the aforementioned drugs (Fig. 6*G*). In contrast, treatments with control vehicle or irrelevant peptide did not inhibit IFN-γ secretion (Fig. 6*G*). Similarly, when secretion of IFN-γ or IL-2 was analyzed by intracellular FACS following treatment of OT-II T cells stimulated with OVA-pulsed DCs with different GJ or Cx43 inhibitors, T cell activation was found impaired in the murine system as well (Supplemental Fig. 4*C–E*). Furthermore, we evaluated the individual contribution of Cx43 from T cells or DCs to the T cell activation process. When GJ activity was inhibited in DCs only, significant reduction of IFN-γ secretion was detected after preincubation with β-Ga or the Cx43-AS ($p < 0.01$ and $p < 0.05$, respectively), but only a slight decrease was obtained after pretreatment with the 1848-mimetic peptide (Fig. 6*H*). In contrast, T cell activation was more dramatically impaired after preincubation of T cells with any of these

Downloaded from http://journals.aai.org/jimmunol/article-pdf/187/6/3121/1348006/1100378.pdf by guest on 10 July 2024

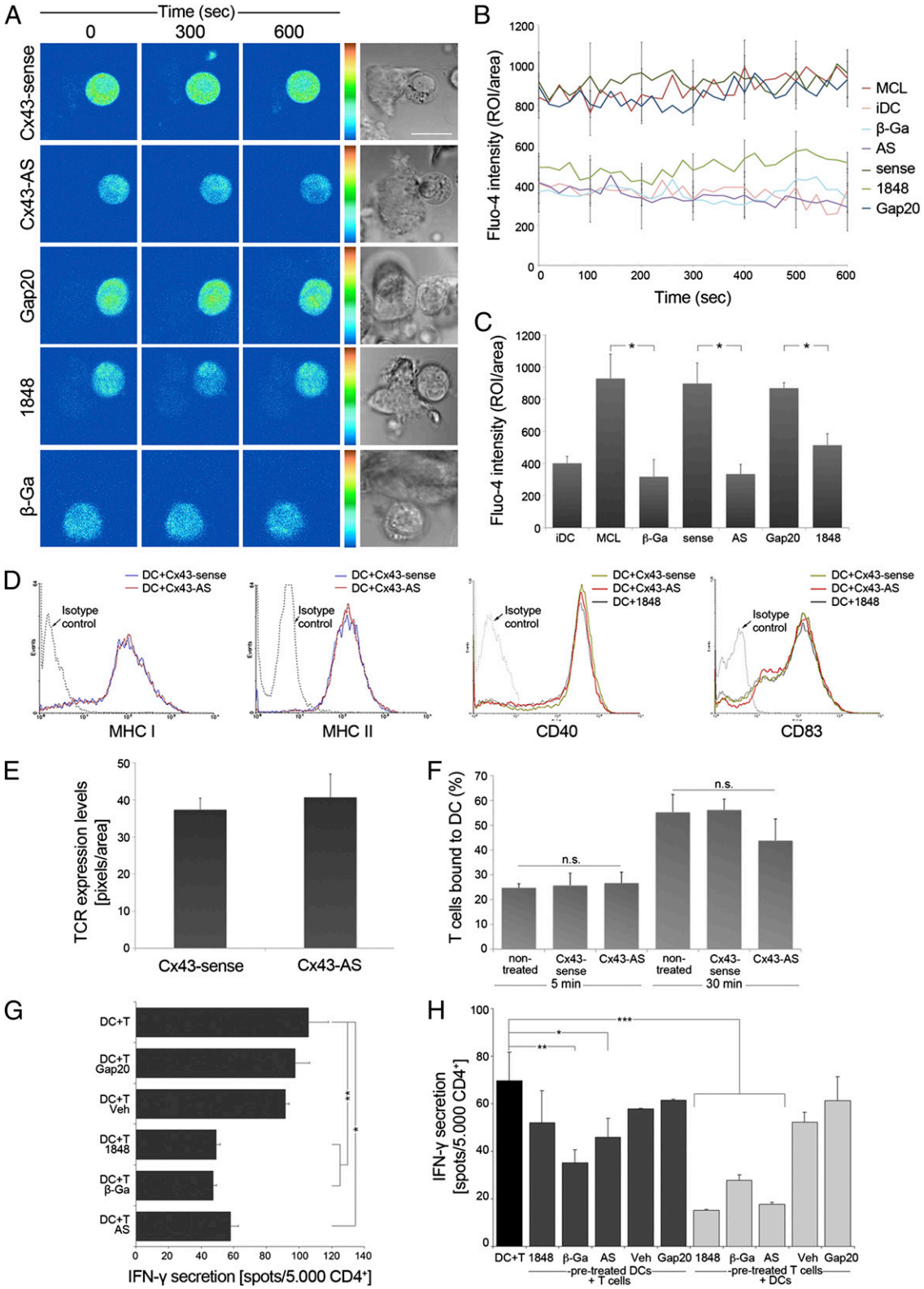

FIGURE 6. Cx43 contributes to T cell activation by DC. *A*, Ca^{2+} signaling was analyzed using Fluo4-AM by sequential confocal images of MCL-specific T cells cocultured with autologous MCL-DCs and treated with different GJs or Cx43 inhibitors and their respective controls. Phase-contrast images corresponding to the same fields are shown. Scale bar, 5 μm. *B*, Time course showing changes of intracellular Ca^{2+} signaling in T cells contacting DCs, under different conditions. Ca^{2+} signals are shown as total mean fluorescence ± SEM. *C*, Overall mean of Fluo4-AM fluorescence over the time ± SEM for each condition ($*p < 0.05$); $n = 3$. *D* and *E*, Treatments with a Cx43-AS or with the 1848 Cx43-mimetic peptide did not affect the expression of MHC class I and class II, CD40, CD83, and TCR. *F*, Cell adhesion was evaluated in conjugates of OVA-DCs and OT-II T cells treated or not with a Cx43-sense or Cx43-AS. Cx43 gene targeting did not affect conjugate formation 5 min and 30 min after DC–T cell coincubation. Each bar represents percentage ± SD of four independent experiments. *G*, IFN-γ secretion was assessed by ELISPOT assay in MCL-specific $CD4^+$ T cells coincubated with MCL-DCs, plus a nonspecific GJ blocker (β-Ga), Cx43-AS, or 1848 Cx43-mimetic peptide. Inhibition of GJIC significantly reduced the secretion of IFN-γ by $CD4^+$ T cells. Data were expressed as the mean of spots/5 × 10^3 effector cells ± SD ($**p < 0.01$, $*p < 0.05$), $n = 2$, performed in triplicate. *H*, MCL-DCs or MCL-

Downloaded from http://journals.aai.org/jimmunol/article-pdf/187/6/3121/1348006/1100378.pdf by guest on 10 July 2024

drugs (Fig. 6*H*, $p < 0.005$). We further investigated IFN-γ secretion in the absence of APCs, following activation with anti-CD3 plus anti-CD28 beads, and after treatment with the 1848-mimetic peptide or a control peptide. IFN-γ secretion was impaired following Cx43-mimetic peptide incubation, but remained unaffected in cells incubated with a control peptide (Supplemental Fig. 4*F*), suggesting a role for Hchl in T cell activation.

Overall, these results suggest a role for GJs and Hchls as coordinators of the DC–T cell signaling machinery that regulates T cell activation.

Discussion

Multiple surface molecules spatially segregated at the IS mediate intercellular communication and activate intracellular signaling pathways, resulting in T cell activation and proliferation. Ag-dependent T cell activation is a cell-cell contact-dependent process, suggesting that mediators of intercellular communication are directly involved. In this study, we have used a combination of experimental approaches to show that Cx43 accumulates at the IS during specific cognate DC–T cell interaction as both GJs and stand-alone Hchls. Redistribution of Cx43 to the IS was Ag specific and time dependent, with maximal accumulation occurring as early as 30 min after DC–T cell conjugate formation, at which time a mature IS has been formed (31). The mature immunological synapse is characterized by a prototypical cSMAC with accumulated MHC:peptide and TCR, among others, surrounded by a pSMAC enriched in molecules such as ICAM-1 and LFA-1 (3, 4). In this study, we found Cx43 accumulated at the pSMAC in T cells and colocalized with LFA-1, which is essential for adhesion and signaling within the IS. Although interactions between opposing Hchls are a form of intercellular adhesion and both adhesion proteins and GJs act in a coordinated fashion to join cells together and allow communication between them (32), silencing of Cx43 did not affect T cell–DC adhesion within the synapse.

Cell surface molecules from all over the T cell membrane are transported to the IS through a mechanism involving the cell cytoskeleton and motor proteins (33). In this study, we show that Cx43 recruitment to the synapse required an intact actin cytoskeleton, as inhibitors of actin polymerization abolished Cx43 accumulation. Although targeting of Cx-Hchls to the plasma membrane, which is essential for GJ formation, involves the microtubule network (27), in our hands inhibition of microtubules did not affect the recruitment of Cx43 to the synapse. Therefore, the Cx43 pool relocated to the IS is not likely to be newly synthesized Cx43, but Cx43 already allocated in the plasma membrane that redistributed to the synapse.

The specific involvement of Cx43 GJ channels in mediating bidirectional communication between DCs and T cells at the IS was demonstrated, and the use of either a GJ drug inhibitor, a specific mimetic peptide, or gene targeting by means of a Cx43-AS oligodeoxynucleotide resulted in blockage of intercellular communication between these cells. Intercellular communication has been previously described between regulatory and effector T lymphocytes (14), follicular DCs and B cells in lymph nodes (34), lymphocytes and endothelial cells (18), and between T cells and B cells (19). Moreover, it was recently shown that GJs mediate communication between macrophages and T lymphocytes, in particular the Th1 cell subset (35), as well as unidirectional communication from DCs to T cells (16), which further reinforces our observations. Cx43 accumulation at the IS and Cx43-mediated T cell–DC functional coupling indicate a direct correlation between both processes, and implicate this protein in mediating signals between these two cell subtypes. The nature of the intracellular signals exchanged through GJs at the synapse is presently unknown, and further studies are required to identify the molecules that travel through GJs formed between DCs and T cells. Whereas GJs form channels that allow direct intercellular communication between adjacent cells, Hchls represent pores formed by a characteristic hexameric assembly of Cx subunits, and mediate communication between cells and their extracellular environment. Even though it has been described that under physiological conditions Hchls composed of Cx43 have a low open probability (29), different reports have demonstrated that they are able to release physiologically relevant quantities of signaling molecules to the extracellular milieu, including NAD^+ and glutamate, and to mediate ATP release that induces intercellular Ca^{2+} signals (36–38).

Activation of T lymphocytes via stimulation of the TCR complex is marked by a rapid and sustained increase of intracellular Ca^{2+}, which is required for gene transcription, cellular proliferation, and differentiation (39). A sustained Ca^{2+} signal for many hours is also necessary to stimulate NFAT, a transcription factor that regulates the expression of various cytokine genes, including IL-2 (39, 40). Different studies have described Cx43 participating in Ca^{2+} influx in various cell types (41). In this work, we presented evidence supporting the participation of Cx43 in regulating Ca^{2+} oscillations in the IS. We demonstrated that specific blockade of Cx43 prevents the sustained rise of intracellular Ca^{2+} that was seen in T cells forming conjugates with Ag-pulsed DCs, in both murine and human models. Cell adhesion is important for the Ca^{2+} flux that is required for T cell activation, but Cx43 gene targeting did not affect adhesion between T cells and DCs, as Cx43 inhibition did not influence the formation of DC–T cell clusters. This result indicates that the reduced Ca^{2+} response seen was the result of inhibition of GJIC rather than of Cx43-mediated cell adhesion.

The increase in intracellular Ca^{2+} is an obligatory step in the cascade of signals that finally results in T cell proliferation (42). Moreover, a role for GJs in T cell activation was recently described, and inhibition of GJIC was responsible for reduced IL-2 secretion and cell proliferation (16). The impaired Ca^{2+} signals we observed as a result of blocking GJs and Cx43 are likely to account for the reduced lymphocyte activation seen after inhibiting GJIC, suggesting that Ca^{2+} signals regulated by GJs may possibly be one of the mechanisms controlling T cell activation. Hchls have also been implicated in controlling sustained proliferation of activated $CD4^+$ T cells (43), and in this study we showed that beside GJs, Cx43 also accumulate at the IS as Hchls, which can regulate Ca^{2+} signaling (44) and mediate ATP release through a mechanism dependent on intracellular Ca^{2+} mobilization (30). Whereas selective blockers for Hchls are not yet known, treatments with a Cx43-mimetic peptide proved Cx43 to be important in regulating Ca^{2+} oscillations. Even though mimetic peptides inhibit intercellular coupling and prevent assembly of newly formed functional GJ channels, some functionality for Cx-Hchls cannot be excluded, as mimetic peptides can also bind to Cx-Hchls, block Hchl docking, and restrict ATP release (45).

Our findings also show that Cx43 participates in the regulation of IFN-γ secretion as both gene targeting of Cx43 and blockade

specific T cells were independently pretreated with β-Ga, 1848-mimetic peptide, Cx43-AS, or their respective controls, and then incubated with nontreated T cells (dark gray) or DCs (light gray), respectively. Control, nontreated T cells, and DCs (black) were also evaluated. Graphic represents IFN-γ secretion reported as the mean of spots/5 × 10^3 $CD4^+$ T cells ± SD (*$p < 0.05$, **$p < 0.01$, ***$p < 0.005$), $n = 2$, performed in triplicate.

Downloaded from http://journals.aai.org/jimmunol/article-pdf/187/6/3121/1348006/1100378.pdf by guest on 10 July 2024

of Cx43-GJ function substantially diminished IFN-γ secretion by primed T cells. In addition, cytokines can positively regulate the surface expression of Cx and GJIC in cells of the immune system (17), suggesting the existence of a positive feedback regulation by cytokines, such as IFN-γ, which can stimulate opening of GJ channels and Cx43 upregulation (13). Such a mechanism may contribute to sustained communication between T cells and APCs, allowing optimal T cell activation. Although we have shown that GJIC is important for T cell activation, we cannot exclude a possible contribution for Hchls to this process. The fact that a Cx43-mimetic peptide has also affected IFN-γ secretion by T cells following incubation with anti-CD3 and anti-CD28 beads suggests that these structures are also involved in T cell activation. This role additionally correlates with our findings of Hchl accumulation at the site of contact between T cells and DCs. As targeting of Cx43 protein expression or the use of a specific Cx43-mimetic peptide blocks boths GJ and Hchl, further studies using Cx43 mutants may provide useful tools to discern the contribution of Hchl to Ag-specific T cell activation.

In summary, this work identifies Cx43 as a key component of the IS and provides evidence of a role for GJ and Hchl in T cell activation, opening new questions regarding the involvement of these structures in the regulation and synchronization of immunological processes.

Acknowledgments

We are particularly grateful to J.C. Sáez for providing specific mAbs and Cx blockers, L. Saragoni and C. Thrasivoulou for confocal support, and M. Briones for technical help. We thank J.C. Sáez, J. Cook, and P. Cormie for critical reading of the manuscript and useful discussions.

Disclosures

The authors have no financial conflicts of interest.

References

1. Babbitt, B. P., P. M. Allen, G. Matsueda, E. Haber, and E. R. Unanue. 1985. Binding of immunogenic peptides to Ia histocompatibility molecules. *Nature* 317: 359–361.
2. Hedrick, S. M., E. A. Nielsen, J. Kavaler, D. I. Cohen, and M. M. Davis. 1984. Sequence relationships between putative T-cell receptor polypeptides and immunoglobulins. *Nature* 308: 153–158.
3. Grakoui, A., S. K. Bromley, C. Sumen, M. M. Davis, A. S. Shaw, P. M. Allen, and M. L. Dustin. 1999. The immunological synapse: a molecular machine controlling T cell activation. *Science* 285: 221–227.
4. Monks, C. R., B. A. Freiberg, H. Kupfer, N. Sciaky, and A. Kupfer. 1998. Three-dimensional segregation of supramolecular activation clusters in T cells. *Nature* 395: 82–86.
5. Trautmann, A., and S. Valitutti. 2003. The diversity of immunological synapses. *Curr. Opin. Immunol.* 15: 249–254.
6. Loewenstein, W. R. 1981. Junctional intercellular communication: the cell-to-cell membrane channel. *Physiol. Rev.* 61: 829–913.
7. Sáez, J. C., J. A. Connor, D. C. Spray, and M. V. Bennett. 1989. Hepatocyte gap junctions are permeable to the second messenger, inositol 1,4,5-trisphosphate, and to calcium ions. *Proc. Natl. Acad. Sci. USA* 86: 2708–2712.
8. Goodenough, D. A. 1975. The structure of cell membranes involved in intercellular communication. *Am. J. Clin. Pathol.* 63: 636–645.
9. Musil, L. S., and D. A. Goodenough. 1991. Biochemical analysis of connexin43 intracellular transport, phosphorylation, and assembly into gap junctional plaques. *J. Cell Biol.* 115: 1357–1374.
10. Oviedo-Orta, E., P. Gasque, and W. H. Evans. 2001. Immunoglobulin and cytokine expression in mixed lymphocyte cultures is reduced by disruption of gap junction intercellular communication. *FASEB J.* 15: 768–774.
11. Zahler, S., A. Hoffmann, T. Gloe, and U. Pohl. 2003. Gap-junctional coupling between neutrophils and endothelial cells: a novel modulator of transendothelial migration. *J. Leukoc. Biol.* 73: 118–126.
12. Neijssen, J., C. Herberts, J. W. Drijfhout, E. Reits, L. Janssen, and J. Neefjes. 2005. Cross-presentation by intercellular peptide transfer through gap junctions. *Nature* 434: 83–88.
13. Matsue, H., J. Yao, K. Matsue, A. Nagasaka, H. Sugiyama, R. Aoki, M. Kitamura, and S. Shimada. 2006. Gap junction-mediated intercellular communication between dendritic cells (DCs) is required for effective activation of DCs. *J. Immunol.* 176: 181–190.
14. Bopp, T., C. Becker, M. Klein, S. Klein-Hessling, A. Palmetshofer, E. Serfling, V. Heib, M. Becker, J. Kubach, S. Schmitt, et al. 2007. Cyclic adenosine monophosphate is a key component of regulatory T cell-mediated suppression. *J. Exp. Med.* 204: 1303–1310.
15. Mendoza-Naranjo, A., P. J. Saéz, C. C. Johansson, M. Ramírez, D. Mandakovic, C. Pereda, M. N. López, R. Kiessling, J. C. Sáez, and F. Salazar-Onfray. 2007. Functional gap junctions facilitate melanoma antigen transfer and cross-presentation between human dendritic cells. *J. Immunol.* 178: 6949–6957.
16. Elgueta, R., J. A. Tobar, K. F. Shoji, J. De Calisto, A. M. Kalergis, M. R. Bono, M. Rosemblatt, and J. C. Sáez. 2009. Gap junctions at the dendritic cell-T cell interface are key elements for antigen-dependent T cell activation. *J. Immunol.* 183: 277–284.
17. Eugenín, E. A., M. C. Brañes, J. W. Berman, and J. C. Sáez. 2003. TNF-alpha plus IFN-gamma induce connexin43 expression and formation of gap junctions between human monocytes/macrophages that enhance physiological responses. *J. Immunol.* 170: 1320–1328.
18. Jara, P. I., M. P. Boric, and J. C. Sáez. 1995. Leukocytes express connexin 43 after activation with lipopolysaccharide and appear to form gap junctions with endothelial cells after ischemia-reperfusion. *Proc. Natl. Acad. Sci. USA* 92: 7011–7015.
19. Oviedo-Orta, E., T. Hoy, and W. H. Evans. 2000. Intercellular communication in the immune system: differential expression of connexin40 and 43, and perturbation of gap junction channel functions in peripheral blood and tonsil human lymphocyte subpopulations. *Immunology* 99: 578–590.
20. López, M. N., C. Pereda, G. Segal, L. Muñoz, R. Aguilera, F. E. González, A. Escobar, A. Ginesta, D. Reyes, R. González, et al. 2009. Prolonged survival of dendritic cell-vaccinated melanoma patients correlates with tumor-specific delayed type IV hypersensitivity response and reduction of tumor growth factor β-expressing T cells. *J. Clin. Oncol.* 27: 945–952.
21. Retamal, M. A., C. J. Cortés, L. Reuss, M. V. Bennett, and J. C. Sáez. 2006. S-nitrosylation and permeation through connexin 43 hemichannels in astrocytes: induction by oxidant stress and reversal by reducing agents. *Proc. Natl. Acad. Sci. USA* 103: 4475–4480.
22. Batista, A., J. Millán, M. Mittelbrunn, F. Sánchez-Madrid, and M. A. Alonso. 2004. Recruitment of transferrin receptor to immunological synapse in response to TCR engagement. *J. Immunol.* 172: 6709–6714.
23. Wright, C. S., D. L. Becker, J. S. Lin, A. E. Warner, and K. Hardy. 2001. Stage-specific and differential expression of gap junctions in the mouse ovary: connexin-specific roles in follicular regulation. *Reproduction* 121: 77–88.
24. Costes, S. V., D. Daelemans, E. H. Cho, Z. Dobbin, G. Pavlakis, and S. Lockett. 2004. Automatic and quantitative measurement of protein-protein colocalization in live cells. *Biophys. J.* 86: 3993–4003.
25. Qiu, C., P. Coutinho, S. Frank, S. Franke, L. Y. Law, P. Martin, C. R. Green, and D. L. Becker. 2003. Targeting connexin43 expression accelerates the rate of wound repair. *Curr. Biol.* 13: 1697–1703.
26. Lippincott-Schwartz, J., E. Snapp, and A. Kenworthy. 2001. Studying protein dynamics in living cells. *Nat. Rev. Mol. Cell Biol.* 2: 444–456.
27. Shaw, R. M., A. J. Fay, M. A. Puthenveedu, M. von Zastrow, Y. N. Jan, and L. Y. Jan. 2007. Microtubule plus-end-tracking proteins target gap junctions directly from the cell interior to adherens junctions. *Cell* 128: 547–560.
28. Dolmetsch, R. E., and R. S. Lewis. 1994. Signaling between intracellular Ca2+ stores and depletion-activated Ca2+ channels generates [Ca2+]i oscillations in T lymphocytes. *J. Gen. Physiol.* 103: 365–388.
29. Contreras, J. E., J. C. Sáez, F. F. Bukauskas, and M. V. Bennett. 2003. Gating and regulation of connexin 43 (Cx43) hemichannels. *Proc. Natl. Acad. Sci. USA* 100: 11388–11393.
30. Cotrina, M. L., J. H. Lin, A. Alves-Rodrigues, S. Liu, J. Li, H. Azmi-Ghadimi, J. Kang, C. C. Naus, and M. Nedergaard. 1998. Connexins regulate calcium signaling by controlling ATP release. *Proc. Natl. Acad. Sci. USA* 95: 15735–15740.
31. Lee, K. H., A. D. Holdorf, M. L. Dustin, A. C. Chan, P. M. Allen, and A. S. Shaw. 2002. T cell receptor signaling precedes immunological synapse formation. *Science* 295: 1539–1542.
32. Hillis, G. S., L. A. Duthie, P. A. Brown, J. G. Simpson, A. M. MacLeod, and N. E. Haites. 1997. Upregulation and co-localization of connexin43 and cellular adhesion molecules in inflammatory renal disease. *J. Pathol.* 182: 373–379.
33. Wülfing, C., and M. M. Davis. 1998. A receptor/cytoskeletal movement triggered by costimulation during T cell activation. *Science* 282: 2266–2269.
34. Krenacs, T., M. van Dartel, E. Lindhout, and M. Rosendaal. 1997. Direct cell/cell communication in the lymphoid germinal center: connexin43 gap junctions functionally couple follicular dendritic cells to each other and to B lymphocytes. *Eur. J. Immunol.* 27: 1489–1497.
35. Bermudez-Fajardo, A., M. Ylihärsilä, W. H. Evans, A. C. Newby, and E. Oviedo-Orta. 2007. CD4+ T lymphocyte subsets express connexin 43 and establish gap junction channel communication with macrophages in vitro. *J. Leukoc. Biol.* 82: 608–612.
36. Bruzzone, S., L. Guida, E. Zocchi, L. Franco, and A. De Flora. 2001. Connexin 43 hemi channels mediate Ca2+-regulated transmembrane NAD+ fluxes in intact cells. *FASEB J.* 15: 10–12.
37. Stout, C. E., J. L. Costantin, C. C. Naus, and A. C. Charles. 2002. Intercellular calcium signaling in astrocytes via ATP release through connexin hemichannels. *J. Biol. Chem.* 277: 10482–10488.
38. Ye, Z. C., M. S. Wyeth, S. Baltan-Tekkok, and B. R. Ransom. 2003. Functional hemichannels in astrocytes: a novel mechanism of glutamate release. *J. Neurosci.* 23: 3588–3596.
39. Lewis, R. S. 2001. Calcium signaling mechanisms in T lymphocytes. *Annu. Rev. Immunol.* 19: 497–521.

Downloaded from http://journals.aai.org/jimmunol/article-pdf/187/6/3121/1348006/1100378.pdf by guest on 10 July 2024

40. Crabtree, G. R. 1999. Generic signals and specific outcomes: signaling through Ca2+, calcineurin, and NF-AT. *Cell* 96: 611–614.
41. Lin, G. C., J. K. Rurangirwa, M. Koval, and T. H. Steinberg. 2004. Gap junctional communication modulates agonist-induced calcium oscillations in transfected HeLa cells. *J. Cell Sci.* 117: 881–887.
42. Jensen, B. S., N. Odum, N. K. Jorgensen, P. Christophersen, and S. P. Olesen. 1999. Inhibition of T cell proliferation by selective block of Ca(2+)-activated K(+) channels. *Proc. Natl. Acad. Sci. USA* 96: 10917–10921.
43. Oviedo-Orta, E., M. Perreau, W. H. Evans, and I. Potolicchio. 2010. Control of the proliferation of activated CD4+ T cells by connexins. *J. Leukoc. Biol.* 88: 79–86.
44. Quist, A. P., S. K. Rhee, H. Lin, and R. Lal. 2000. Physiological role of gap-junctional hemichannels: extracellular calcium-dependent isosmotic volume regulation. *J. Cell Biol.* 148: 1063–1074.
45. Evans, W. H., E. De Vuyst, and L. Leybaert. 2006. The gap junction cellular internet: connexin hemichannels enter the signalling limelight. *Biochem. J.* 397: 1–14.

Downloaded from http://journals.aai.org/jimmunol/article-pdf/187/6/3121/1348006/1100378.pdf by guest on 10 July 2024